Evidence for Large Increases in Clear-Air Turbulence Over the Past Four Decades

Mark C. Prosser[1] [iD], Paul D. Williams[1] [iD], Graeme J. Marlton[2], and R. Giles Harrison[1] [iD]

[1]Department of Meteorology, University of Reading, Reading, UK, [2]The UK Meteorological Office, Exeter, UK

Abstract Clear-air turbulence (CAT) is hazardous to aircraft and is projected to intensify in response to future climate change. However, our understanding of past CAT trends is currently limited, being derived largely from outdated reanalysis data. Here we analyze CAT trends globally during 1979–2020 in a modern reanalysis data set using 21 diagnostics. We find clear evidence of large increases around the midlatitudes at aircraft cruising altitudes. For example, at an average point over the North Atlantic, the total annual duration of light-or-greater CAT increased by 17% from 466.5 hr in 1979 to 546.8 hr in 2020, with even larger relative changes for moderate-or greater CAT (increasing by 37% from 70.0 to 96.1 hr) and severe-or-greater CAT (increasing by 55% from 17.7 to 27.4 hr). Similar increases are also found over the continental USA. Our study represents the best evidence yet that CAT has increased over the past four decades.

Plain Language Summary Turbulence is unpleasant to fly through in an aircraft. Strong turbulence can even injure air passengers and flight attendants. An invisible form called clear-air turbulence (CAT) is predicted to become more frequent because of climate change. Here we analyze modern atmospheric data based on four decades of observations (1979–2020) to investigate whether CAT has already started to increase. We use 21 different turbulence calculations to ensure our results are as reliable as possible. We find clear evidence of large CAT increases in various places around the world at aircraft cruising altitudes since satellites began observing the atmosphere. For example, at a typical point over the North Atlantic, the upward trend is such that the strongest category of CAT was 55% more frequent in 2020 than 1979. Our study represents the best evidence yet that CAT has increased over the past four decades, consistent with the expected effects of climate change.

1. Introduction

Turbulence is estimated to cost the aviation industry around US$200 million annually in the USA alone (Eichenbaum, 2003). These costs arise partly from additional airframe fatigue, requiring maintenance and subsequent loss of productivity, as well as occasional airframe damage. Additionally, passengers and crew suffer injuries, some requiring costly hospital treatment. Some aircraft turbulence occurs in well-defined locations, such as over mountain ranges or within the vicinity of convective storms, and is largely avoidable. However, clear-air turbulence (CAT) is difficult to observe in advance of an aircraft's track using remote sensing methods. Furthermore, it is still challenging for aviation meteorologists to forecast CAT, partly because current Numerical Weather Prediction (NWP) models have grid sizes that are many times larger than the turbulent eddies that affect aircraft. Hence, operational forecasters use empirical turbulence diagnostics (e.g., Brown, 1973; Dutton, 1980; Ellrod & Knapp, 1992; Knox, 1997; Knox et al., 2008; McCann et al., 2012) calculated from the temperature and wind fields of NWP output. In recent years, these diagnostics have been combined into multi-diagnostic forecasts (Sharman et al., 2006).

Williams and Joshi (2013) applied 21 CAT diagnostics to the 200 hPa pressure surface (corresponding to a flight level of approximately 39,000 ft) of a climate model using a doubled-CO_2 scenario. They found that the future occurrence of moderate-or-greater (MOG) CAT increased substantially during winter in the North Atlantic. MOG CAT is defined by the Federal Aviation Administration (FAA, 2006) as the point at which unsecured objects begin to move, and at which people find it difficult to move around inside the cabin. Williams (2017) expanded the analysis to examine turbulence increases at different severity levels (light, moderate, and severe) and found an increase in the frequency of diagnosed CAT for nearly all threshold–diagnostic pairs. Storer et al. (2017) analyzed a CMIP5 simulation using the RCP8.5 scenario in 2050–2080 and compared it with a pre-industrial control simulation, covering the whole globe and each season at different flight levels. Within the jet stream

regions of both hemispheres, the RCP8.5 scenario relative to the pre-industrial control showed around a 300% increase in CAT.

S. H. Lee et al. (2019) examined three reanalysis datasets over 1979–2017 and found evidence of a 15% increase in vertical wind shear strength at 250 hPa over the North Atlantic (30–70°N, 10–80°W). As is well known, when the ratio of thermal stability to vertical wind shear (Richardson number Ri) is less than some critical value, typically 0.25, Kelvin–Helmholtz instabilities can form and ultimately result in CAT. Therefore, stronger vertical wind shear is expected to increase the amount of turbulence. However, studies examining whether the amount of CAT measured by aircraft has increased due to recent warming trends are limited by the availability of suitable data. The record of automated, quantitative eddy dissipation rate (EDR) turbulence measurements is too short. Pilot reports (PIREPs) have a longer record, but are not quantitative, and the geographical distribution of CAT based on PIREPs is limited in spatial and temporal extent (Wolff & Sharman, 2008). Furthermore, long-term improvements in operational CAT forecast skill should be acting to reduce the probability of encountering turbulence, even if the amount of turbulence in the atmosphere is increasing.

Outside aviation, CAT is also of interest as a mechanism allowing the mixing of air between the troposphere and stratosphere. Jaeger and Sprenger (2007; hereafter JS07) used ERA40 reanalysis data (Uppala et al., 2005) to compute a winter and summer northern hemisphere CAT climatology (1958–2001) near the dynamic tropopause, using four CAT diagnostics: Richardson number, negative squared Brunt–Väisäla frequency, negative potential vorticity (Gidel & Shapiro, 1979), and Ellrod's turbulence index (Ellrod & Knapp, 1992). An increase in all four of these indices over the north Atlantic, European, and US regions was found. However, for aviation purposes, aircraft fly along constant flight levels as opposed to the dynamic tropopause. Furthermore, the first 22 years of JS07's climatology uses reanalysis data from before the start of meteorological satellite era in 1979, leading to data quality concerns. Marlton et al. (2021) and Simmons et al. (2020) showed that the commissioning and decommissioning of meteorological satellites can introduce biases. J. H. Lee et al. (2023) have recently updated JS07's work (see Section 4 for a discussion).

Renalysis packages now contain four decades of data entirely in the satellite era, during which the world has continued to warm. Therefore, the present study aims to analyze CAT trends during 1979–2020 in the ERA5 reanalysis data set, which has more advanced model physics and higher vertical and horizontal resolution than ERA40. The 21 diagnostics used in Williams and Joshi (2013) and Williams (2017) will be computed, as opposed to the four in JS07, to yield an improved quantification of inter-diagnostic uncertainties. These 21 diagnostics have previously been validated using aircraft measurements of CAT and have generally been found to be skillful (e.g., Sharman et al., 2006). To make the results more applicable to global aviation, the diagnostics will be calculated on the 197 hPa pressure level, corresponding approximately to a flight level of 39,000 ft (FL390), rather than the tropopause, and for the entire globe as opposed to just the northern hemisphere considered by JS07 and J. H. Lee et al. (2023).

The layout of this paper is as follows. Section 2 describes a methodology to compute the number of times a year a given turbulence severity occurs. Section 3 presents the results. Section 4 concludes with a discussion and summary.

2. Methodology

Global ERA5 reanalysis data (Hersbach et al., 2020) containing zonal and meridional wind speed, dry bulb temperature, and geopotential height were extracted on the 197 hPa pressure level with 0.25° horizontal resolution at three hourly intervals from 1 January 1979 to 31 December 2020. To allow the computation of CAT diagnostics that require vertical derivatives, fields on the 188 and 206 hPa levels were also extracted. The 21 turbulence diagnostics were then calculated from the extracted reanalysis fields every three hours.

To allow an inter-diagnostic comparison, the uncalibrated CAT diagnostic values, each with different physical units, are compared with threshold values derived from a climatological probability distribution for each diagnostic, following Williams (2017). The reanalysis data were extracted on a fixed Gaussian grid, meaning more data points for a given surface area near the pole than the equator, and so the climatological probability distributions were latitudinally weighted. The latitudinally weighted distributions were calculated for the year 2000, a reference year chosen as being the 1979–2020 midpoint.
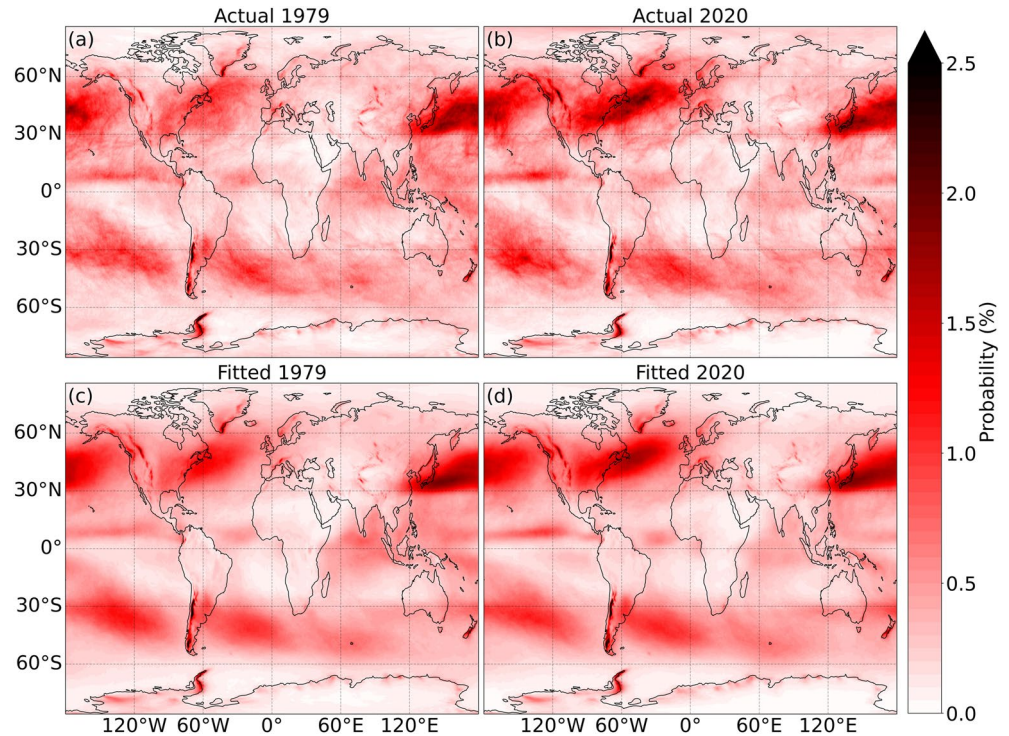
Figure 1. Annual-mean probabilities of encountering moderate-or-greater clear-air turbulence (CAT) in (a) the year 1979, (b) the year 2020, (c) the year 1979 inferred from the linear regression model, and (d) the year 2020 inferred from the linear regression model. The probabilities are calculated from ERA5 at 197 hPa and are averaged over 21 CAT diagnostics. See Supporting Information S1 for light-or-greater and severe-or-greater CAT versions of this figure.

Following Williams (2017), the diagnostic values corresponding to the 97th, 99.1st, 99.6th, 99.8th, and 99.9th percentiles were then derived globally for the reference year 2000, corresponding, respectively, to the thresholds for light-or-greater (LOG), light-to-moderate-or-greater (LMOG), moderate-or-greater (MOG), moderate-to-severe-or-greater (MSOG), and severe-or-greater (SOG) turbulence. For each diagnostic and threshold, the number of exceedances at a given coordinate for each month, season, and year in the study period were computed. For each year, an average exceedance field was calculated by taking the mean of the 21 exceedance fields for each diagnostic.

To calculate temporal trends, linear regression was applied at each grid point using the annual-mean exceedance values for the 1979–2020 period for the five turbulence severities. Using the regression model at each grid point, fitted 1979 and 2020 exceedances were computed as a guide to the underlying turbulence statistics in the absence of interannual variability at the start and end of the period. In the rare cases that these fitted exceedances were negative, they were set to zero. Exceedances were converted into percentage probabilities of exceedance, by normalizing by the number of three-hour periods in each year.

Absolute changes in the probability of encountering turbulence over the 42 years were computed by subtracting the fitted 1979 values from the fitted 2020 values. For example, a 1% increase over one year would be equivalent to around 29 extra exceedances, given the 2,920 three-hour periods in a single year. To calculate the relative changes, the absolute changes were divided by the fitted 1979 values and multiplied by 100, to yield a percentage relative change.

3. Results

Figure 1 shows global maps of the annual-mean diagnostic-mean MOG CAT probability in 1979 and 2020. The spatial structures of the probabilities inferred from the linear regression model are smoother than the raw annual fields, because interannual variability has been filtered out. The probability of diagnosed MOG CAT is generally larger over the oceans than the continents and is larger in the midlatitudes where the atmospheric jet streams are
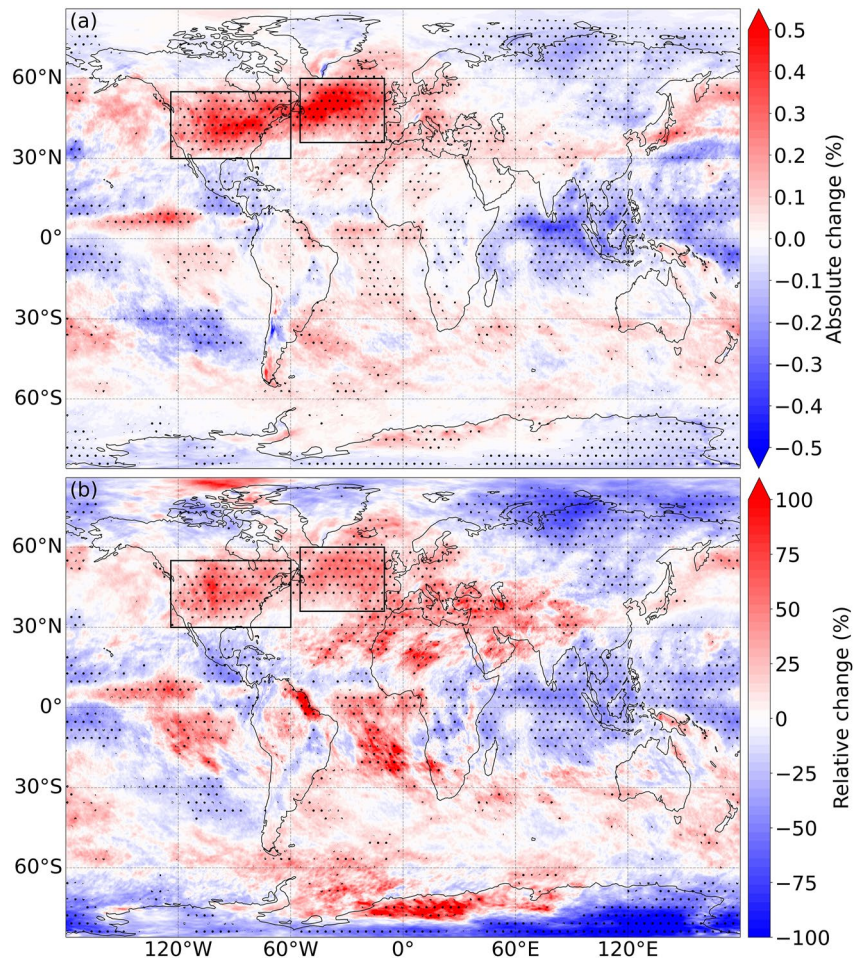
Figure 2. The change in ERA5's 197 hPa annual-mean diagnostic-mean moderate-or-greater (MOG) clear-air turbulence (CAT) probability over 1979–2020, showing (a) the absolute change and (b) the relative change. The changes are diagnosed from the linear trend. Stippling indicates statistical significance at the $p = 0.05$ level, according to a two-sided Wald test (Fahrmeir et al., 2022) applied to the absolute change. The two boxes represent the North Atlantic (36–60°N and 55–10°W) and USA (30–55°N and 124–60°W) areas used in Figures 3 and 4 and Table 1. See Supporting Information S1 for light-or-greater and severe-or-greater CAT versions of this figure as well as a breakdown by diagnostic for the absolute change to MOG CAT.

located. A band of diagnosed MOG CAT is also evident along the equatorial oceans, as discussed in Williams and Storer (2022). The probability of MOG CAT in the Northern Hemisphere midlatitudes (30–60°N) is roughly double the corresponding probability in the Southern Hemisphere (30–60°S). Mountainous regions such as the Andes and Rockies have higher probabilities of MOG CAT, possibly due to mountain wave breaking.

Figure 2a shows the absolute change in the probability of MOG CAT from 1979 to 2020. In the North Atlantic sector, the diagnosed MOG CAT probability has increased by 0.3% in absolute terms, implying an extra 26 hr per year of diagnosed MOG CAT over the entire 42-year period, equivalent to an annual increment of around 40 min. A smaller increase is evident over the northern Pacific, but it is less pronounced. Figure 2b shows the corresponding relative change in the probability of MOG CAT from 1979 to 2020. Regions over the USA and the North Atlantic exhibit relative increases of up to 100%, indicating that both the absolute and relative changes over the period have been large. Other areas such as northern Brazil and parts of the coast of Antarctica also show large relative increases, despite the absolute increases being more modest. In addition to the large changes seen over the USA and the North Atlantic, there are also statistically significant changes over Europe and the Middle East, as well as the South Atlantic and Eastern Pacific.

Figure 3 shows the annual probabilities of diagnosed MOG CAT for each year in the period 1979–2020 over the North Atlantic and USA, averaged over all diagnostics. There is a large increasing trend in both regions. For example,
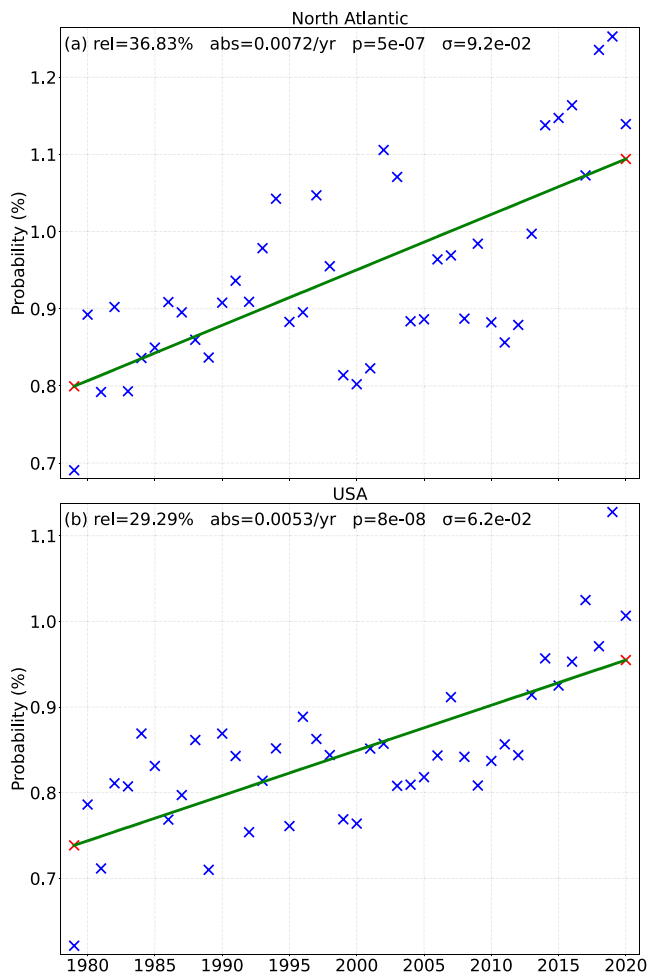
Figure 3. A linear regression analysis conducted on the ERA5 197 hPa annual-mean diagnostic-mean moderate-or-greater clear-air turbulence (CAT) probability for the (a) North Atlantic and (b) USA boxes indicated in Figure 2. The 42 blue crosses in each panel indicate data from the 42 years, whereas the two red crosses show the fitted 1979 and 2020 values. Stated at the top of each panel are the relative change in the fit from 1979 to 2020 (%), the absolute change per year calculated as the slope of the regression line (%/yr), the p value for the slope, and the standard deviation of the residual (σ; %). See Supporting Information S1 for light-or-greater and severe-or-greater CAT versions of this figure.

the North Atlantic starts at an absolute probability of 0.8% in 1979 and increases by 37% (in relative terms) to an absolute probability of nearly 1.1% in 2020. This increase equates to more than a whole day's worth of additional diagnosed MOG CAT exceedances per year in 2020 relative to 1979. The interannual variations in turbulence are noticeably greater in the North Atlantic than the USA, possibly because of the influence of the North Atlantic Oscillation (NAO); see Kim et al. (2016, 2020). Note that, over the 42-year period, the average latitude of the subpolar jet may have shifted, but this shift is negligible compared to the latitudinal extent of these boxes (Archer & Caldeira, 2008; Simmons, 2022).

Figure 4 expands on the North Atlantic analysis in Figure 3a by decomposing it into the 21 constituent CAT diagnostics. It is seen that 17 of the 21 diagnostics show significant ($p < 0.05$) upward trends, with relative changes of up to 75.6%. The remaining 4 diagnostics show no significant trend, and none of the diagnostics shows a significant downward trend. These results indicate a high level of inter-diagnostic agreement that MOG CAT increased over the study period.

Table 1 shows the absolute and relative changes in hours of diagnosed CAT averaged in the North Atlantic, broken down by season and turbulence severity. There is a seasonal cycle, with autumn and winter having more CAT (of all strengths) than spring and summer, because of the seasonal cycle in jet stream strength. The number of hours spent in turbulence generally decreases with increasing turbulence strength, because climatologically stronger turbulence is rarer. For LOG CAT, annually there were 466.5 hr of turbulence in 1979, increasing by 80.2 hr (17%) to 546.8 hr in 2020. In contrast, the relative increases are generally larger with increasing turbulence strength, consistent with the future projections of Williams (2017). For SOG CAT annually, there were 17.7 hr of turbulence in 1979, increasing by 9.7 hr (55%) to 27.4 hr in 2020.

4. Summary and Discussion

In this paper, trends in ERA5's 21-diagnostic-averaged CAT probability at 197 hPa over the period 1979–2020 were examined. The largest increases in both absolute and relative MOG CAT were found over the North Atlantic and continental United States, with statistically significant absolute increases of 0.3% (26 hr) and 0.22% (19 hr), respectively, over the total reanalysis period. Absolute changes are important in regard to aircraft damage, as every additional minute spent traversing turbulence causes fatigue and increases wear-and-tear on the airframe and increases maintenance costs and the potential for injuries, irrespective of whether the increase is on top of a low or high base rate.

The above two hotspots for increased CAT contrast with the East Asian and East Pacific hotspots identified by J. H. Lee et al. (2023). There is an important methodological difference between our studies, in addition to the different seasons and diagnostics used, that may account for these different results. This difference likely arises because many CAT diagnostics require the computation of vertical derivatives. To compute these derivatives, we used input fields at 206 hPa and 188 hPa to calculate the diagnostic values at 197 hPa. In contrast, J. H. Lee et al. (2023) appear to have used input fields at 200 hPa and 300 hPa to calculate the diagnostic values at 250 hPa. This means we have used much finer (and therefore more accurate) vertical finite differences to compute the gradients. Interestingly, of all the CAT diagnostics that the studies have in common, the two that do not require the computation of a vertical derivative (namely the deformation and divergence) are very similar between the two studies, lending support to this explanation for the differences. In this paper we have also examined 21 diagnostics, many more than J. H. Lee et al. (2023), and we have examined the whole globe rather than just the northern extra-tropics (20–60°N).

The corresponding relative increases for the end of the reanalysis period compared to the start are 37% for the North Atlantic and 29% for the USA. These relative changes are useful for diagnosing which regions are expected to become significantly more turbulent. For example, Figure 2b shows that over the northern coast of Brazil there
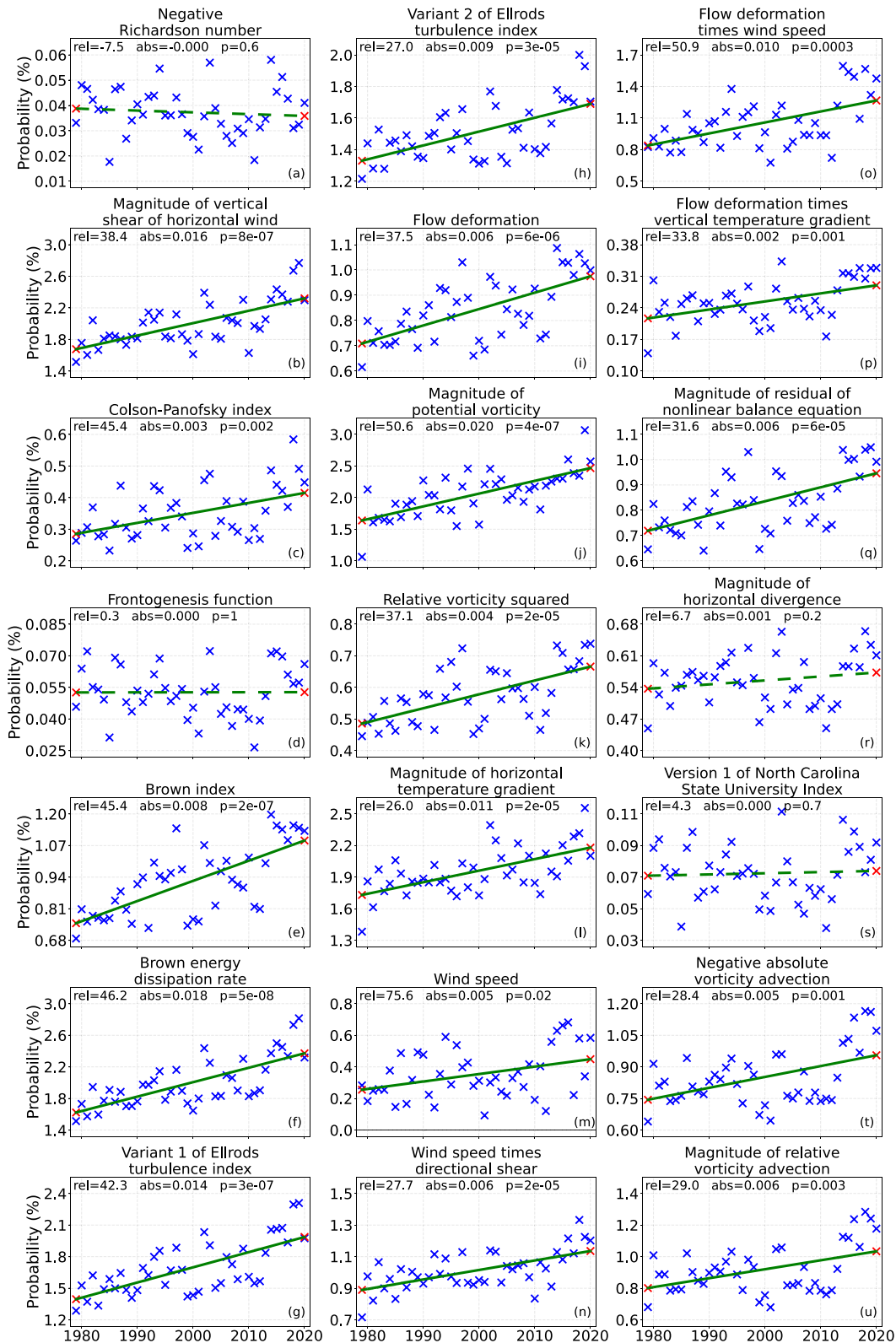
Figure 4. A linear regression analysis conducted on the ERA5 197 hPa annual-mean moderate-or-greater clear-air turbulence (CAT) probability for the North Atlantic box indicated in Figure 2, for each of the 21 CAT diagnostics. The 42 blue crosses in each panel indicate data from the 42 years, whereas the two red crosses show the fitted 1979 and 2020 values. Solid (dashed) green lines indicate trends that are (are not) statistically significant at the $p = 0.05$ level, according to a two-sided Wald test. Stated at the top of each panel are the relative change in the fit from 1979 to 2020 (%), the absolute change calculated as the slope of the regression line (%/yr), and the p value for the slope. See Supporting Information S1 for light-or-greater and severe-or-greater CAT versions of this figure.

Table 1
Fitted Changes From 1979 to 2020 in the Number of Hours (Per Season and Annually) Spent in Clear-Air Turbulence, Derived From ERA5 at 197 hPa Using a Diagnostic-Mean Calculation, for an Average Point in the North Atlantic Box Indicated in Figure 2

Season	Threshold	LOG	LMOG	MOG	MSOG	SOG
DJF	1979 turbulence (h)	128.9	45.6	22.3	12.1	6.4
	2020 turbulence (h)	155.6	59.3	30.6	17.2	9.6
	Absolute increase (h)	26.7	13.7	8.3	5.2	3.1
	Relative increase (%)	21	30	37	43	49
MAM	1979 turbulence (h)	90.4	27.2	11.8	5.7	2.7
	2020 turbulence (h)	113.4	38.9	18.6	9.7	5.0
	Absolute increase (h)	23.1	11.7	6.8	4.0	2.3
	Relative increase (%)	26	43	57	71	85
JJA	1979 turbulence (h)	114.1	36.5	16.1	7.7	3.6
	2020 turbulence (h)	124.5	43.8	21.1	10.9	5.5
	Absolute increase (h)	10.4	7.3	5.0	3.2	1.9
	Relative increase (%)	9	20	31	41	52
SON	1979 turbulence (h)	133.1	43.4	19.8	10.0	5.0
	2020 turbulence (h)	153.2	53.4	25.8	13.9	7.4
	Absolute increase (h)	20.1	10.0	6.0	3.9	2.4
	Relative increase (%)	15	23	31	39	47
Annual	1979 turbulence (h)	466.5	152.7	70.0	35.5	17.7
	2020 turbulence (h)	546.8	195.4	96.1	51.8	27.4
	Absolute increase (h)	80.2	42.7	26.1	16.3	9.7
	Relative increase (%)	17	28	37	46	55

Note. The changes are broken down by season for five turbulence strength thresholds: LOG, light-or-greater; LMOG, light-to-moderate-or-greater; MOG, moderate-or-greater; MSOG, moderate-to-severe-or-greater; and SOG, severe-or-greater. The changes are statistically significant for each combination of season and threshold ($p < 3 \times 10^{-2}$ in all cases).

is a 100% relative increase in MOG CAT, which informs us that even though the baseline occurrence is relatively low compared to other regions, the frequency has now doubled compared to the start of the period. This is of great importance, as these regions cover some of the globe's busiest flight corridors. Our study represents the best evidence yet that CAT has increased over the past four decades.

Regions over western ocean basins are hot spots for diagnosed CAT. This is partly because jet streams tend to be fastest over the ocean, due to the low surface roughness compared to the land. It is also partly because there is a large zonal temperature contrast between the ocean and continent at the western boundary, especially in winter, due to their different specific heat capacities. These horizontal temperature gradients contribute to vertical wind shear, which in turn contribute to CAT.

Future CAT projections by Williams and Joshi (2013) and Williams (2017) using climate models showed increases over the North Atlantic region in DJF for a doubling of CO_2 relative to a pre-industrial control run (560 and 280 ppm CO_2, respectively). For example, an average across Williams and Joshi's 21 diagnostics gives an 83.9% increase in MOG CAT occurrence for doubled CO_2. During the 1979–2020 period, CO_2 concentrations rose by around 30% (from 335 to 410 ppm), yet our study finds a CAT increase of 37% in this region and season over this period, which (after accounting for the different CO_2 rises) is more than we would expect from the climate model results. Williams and Storer (2022) also observed greater CAT increases in reanalysis data than a climate model. Taken together, these findings suggest that climate model simulations may underestimate future CAT increases. Our analysis has used ERA5.1, which corrects for the known cold bias in the lower stratosphere during 2000–2006 in the previous version of ERA5 (Simmons et al., 2020). As with all reanalysis datasets, the quality and quantity of assimilated observational data generally improve over time, although ERA5 has good multidecadal consistency with the plentiful wind observations from aircraft and satellites near the tropopause (Simmons, 2022).

Future work should address the limitations of this study. The sensitivity of the results to using an equally weighted ensemble mean of CAT diagnostics should be explored. Trends in other forms of aviation-affecting turbulence apart from CAT, including convectively induced turbulence (CIT) and mountain wave turbulence (MWT), should be diagnosed from forthcoming reanalysis datasets, such as the planned ERA6 that will contain various convection diagnostics. The northern hemisphere's greater positive trend than the southern hemisphere also warrants further investigation. Turbulence data from aircraft could also be analyzed, but the time period for which quantitative, automated measurements are available is far shorter than the 42 years covered here, making trend detection problematic. In the absence of a long-term record of quantitative aircraft turbulence measurements, reanalysis diagnostics provide the best available global picture of historic variations in CAT.

Data Availability Statement

This paper made extensive use of meteorological data from the ERA5 reanalysis data set from the ECMWF's MARS archive. ERA5 can be downloaded here: https://apps.ecmwf.int/data-catalogues/era5/?class=ea. Registration is required.
An example ERA5 retrieval for July 2016 is given below: RETRIEVE,
CLASS = EA,
TYPE = AN,
STREAM = OPER,
EXPVER = 0001,

REPRES = SH,
LEVTYPE = ML,
LEVELIST = 1/TO/137,
PARAM = 129/152/130/133/135/138/155,
DATE = 20160701/TO/20160731,
TIME = 0000/0300/0600/0900/1200/1500/1800/2100,
STEP = 00,
TARGET = "ERA5_global_raw_[date].grib."

References

Archer, C. L., & Caldeira, K. (2008). Historical trends in the jet streams. *Geophysical Research Letters*, *35*(8), L08803. https://doi.org/10.1029/2008gl033614

Brown, R. (1973). New indexes to locate clear-air turbulence. *Meteorological Magazine*, *102*(1217), 347–361.

Dutton, M. (1980). Probability forecasts of clear-air turbulence based on numerical model output. *Meteorological Magazine*, *109*(1299), 293–310.

Eichenbaum, H. (2003). Historical overview of turbulence accidents and case study analysis. MCR Federal Inc. Rep. Br-M021/080–1 (82 pp.).

Ellrod, G. P., & Knapp, D. I. (1992). An objective clear-air turbulence forecasting technique: Verification and operational use. *Weather and Forecasting*, *7*(1), 150–165. https://doi.org/10.1175/1520-0434(1992)007<0150:aocatf>2.0.co;2

FAA. (2006). *Preventing injuries caused by turbulence*. Advisory circular 120-88A. Federal Aviation Administration.

Fahrmeir, L., Kneib, T., Lang, S., & Marx, B. D. (2022). Regression models. In *Regression: Models, methods and applications* (pp. 23–84). Springer.

Gidel, L. T., & Shapiro, M. A. (1979). The role of clear air turbulence in the production of potential vorticity in the vicinity of upper tropospheric jet stream-frontal systems. *Journal of the Atmospheric Sciences*, *36*(11), 2125–2138. https://doi.org/10.1175/1520-0469(1979)036<2125:trocat>2.0.co;2

Hersbach, H., Bell, B., Berrisford, P., Hirahara, S., Horányi, A., Muñoz-Sabater, J., et al. (2020). The ERA5 global reanalysis. *Quarterly Journal of the Royal Meteorological Society*, *146*(730), 1999–2049. https://doi.org/10.1002/qj.3803

Jaeger, E. B., & Sprenger, M. (2007). A Northern Hemispheric climatology of indices for clear air turbulence in the tropopause region derived from ERA40 reanalysis data. *Journal of Geophysical Research*, *112*(D20), D20106. https://doi.org/10.1029/2006jd008189

Kim, J. H., Chan, W. N., Sridhar, B., Sharman, R. D., Williams, P. D., & Strahan, M. (2016). Impact of the North Atlantic Oscillation on transatlantic flight routes and clear-air turbulence. *Journal of Applied Meteorology and Climatology*, *55*(3), 763–771. https://doi.org/10.1175/jamc-d-15-0261.1

Kim, J. H., Kim, D., Lee, D. B., Chun, H. Y., Sharman, R. D., Williams, P. D., & Kim, Y. J. (2020). Impact of climate variabilities on trans-oceanic flight times and emissions during strong NAO and ENSO phases. *Environmental Research Letters*, *15*(10), 105017. https://doi.org/10.1088/1748-9326/abaa77

Knox, J. A. (1997). Possible mechanisms of clear-air turbulence in strongly anticyclonic flows. *Monthly Weather Review*, *125*(6), 1251–1259. https://doi.org/10.1175/1520-0493(1997)125<1251:pmocat>2.0.co;2

Knox, J. A., McCann, D. W., & Williams, P. D. (2008). Application of the Lighthill–Ford theory of spontaneous imbalance to clear-air turbulence forecasting. *Journal of the Atmospheric Sciences*, *65*(10), 3292–3304. https://doi.org/10.1175/2008jas2477.1

Lee, J. H., Kim, J. H., Sharman, R. D., Kim, J., & Son, S. W. (2023). Climatology of clear-air turbulence in upper troposphere and lower stratosphere in the Northern Hemisphere using ERA5 reanalysis data. *Journal of Geophysical Research: Atmospheres*, *128*(1), 2022JD037679. https://doi.org/10.1029/2022jd037679

Lee, S. H., Williams, P. D., & Frame, T. H. A. (2019). Increased shear in the North Atlantic upper-level jet stream over the past four decades. *Nature*, *572*(7771), 639–642. https://doi.org/10.1038/s41586-019-1465-z

Marlton, G., Charlton-Perez, A., Harrison, G., Polichtchouk, I., Hauchecorne, A., Keckhut, P., et al. (2021). Using a network of temperature lidars to identify temperature biases in the upper stratosphere in ECMWF reanalyses. *Atmospheric Chemistry and Physics*, *21*(8), 6079–6092. https://doi.org/10.5194/acp-21-6079-2021

McCann, D. W., Knox, J. A., & Williams, P. D. (2012). An improvement in clear-air turbulence forecasting based on spontaneous imbalance theory: The ULTURB algorithm. *Meteorological Applications*, *19*(1), 71–78. https://doi.org/10.1002/met.260

Sharman, R., Tebaldi, C., Wiener, G., & Wolff, J. (2006). An integrated approach to mid- and upper-level turbulence forecasting. *Weather and Forecasting*, *21*(3), 268–287. https://doi.org/10.1175/waf924.1

Simmons, A. J. (2022). Trends in the tropospheric general circulation from 1979 to 2022. *Weather and Climate Dynamics*, *3*(3), 777–809. https://doi.org/10.5194/wcd-3-777-2022

Simmons, A. J., Soci, C., Nicolas, J., Bell, B., Berrisford, P., Dragani, R., et al. (2020). *Global stratospheric temperature bias and other stratospheric aspects of ERA5 and ERA5.1*. ECMWF technical memoranda 859. ECMWF.

Storer, L. N., Williams, P. D., & Joshi, M. M. (2017). Global response of clear-air turbulence to climate change. *Geophysical Research Letters*, *44*(19), 9976–9984. https://doi.org/10.1002/2017gl074618

Uppala, S. M., Kållberg, P., Simmons, A. J., Andrae, U., Bechtold, V. D. C., Fiorino, M., et al. (2005). The ERA-40 re-analysis. *Quarterly Journal of the Royal Meteorological Society*, *131*(612), 2961–3012. https://doi.org/10.1256/qj.04.176

Williams, P. D. (2017). Increased light, moderate, and severe clear-air turbulence in response to climate change. *Advances in Atmospheric Sciences*, *34*(5), 576–586. https://doi.org/10.1007/s00376-017-6268-2

Williams, P. D., & Joshi, M. M. (2013). Intensification of winter transatlantic aviation turbulence in response to climate change. *Nature Climate Change*, *3*(3), 644–648. https://doi.org/10.1038/nclimate1866

Williams, P. D., & Storer, L. N. (2022). Can a climate model successfully diagnose clear-air turbulence and its response to climate change? *Quarterly Journal of the Royal Meteorological Society*, *148*(744), 1424–1438. https://doi.org/10.1002/qj.4270

Wolff, J., & Sharman, R. (2008). Climatology of upper-level turbulence over the contiguous United States. *Journal of Applied Meteorology and Climatology*, *47*(8), 2198–2214. https://doi.org/10.1175/2008jamc1799.1